

A-2-2

NUMERICAL INVESTIGATION OF A RIDGED WAVEGUIDE PHASED ARRAY IN AN EQUILATERAL TRIANGULAR ARRANGEMENT

Seiji Mano, Makoto Ono, and Motoo Mizusawa

Mitsubishi Electric Corporation
Kamimachiya, Kamakura City, Japan 247

Introduction

Due to its wideband properties and reduced size, an open-ended ridged waveguide has been used as a phased array element for wideband and wide angle scanning. Montgomery [1] has applied the complete solution [2] of ridged waveguide to a phased array boundary value problem and shown that wide band matching can be done for a particular size of ridged waveguide element. The work of Wang et al. [2] has been a parametric study in the case of ultra wideband of 40% and 58%.

Depending on the numerical method [1], this paper is directed to make clear some fundamental effects of ridge insertion on the unmatched aperture performance of a rectangular double ridged waveguide element in an equilateral triangular arrangement.

Array and Waveguide Parameters

Figure 1 shows double ridged waveguide elements in an equilateral triangular arrangement. We deal with a horizontal arrangement only as in Fig.1 due to its less difficulty of matching than a vertical one [4]. The geometry of a double ridged waveguide is shown in Fig.2. If a phased array of Fig.1 has a conical scan coverage of θ_M with respect to its normal (z-axis) and a 5% reduction [4] of dx and dy is adopted, we may write

$$dx = 0.95 \left(\frac{2\lambda}{1 + \sin \theta_M} \right) \quad (1)$$

and

$$dy = dx/\sqrt{3} \quad (2)$$

where λ is the free space wavelength. From Fig.1 the dimension a_2 should be

$$a_2 \leq (dx/2) - w \quad (3)$$

and a_4 is set here as an upper limit

$$a_4 = (dy/4) - w \quad (4)$$

Also, it is assumed as $a_1/a_2=0.2$ and $w = \lambda/20$. Letting f and f_{c1} be the operating frequency and the cutoff frequency of a dominant waveguide mode, respectively, we impose the condition

$$f_{c1}/f = 0.7 \quad (5)$$

on the parameters a_2 and a_3 . In determining eigenvalues of ridged waveguide modes by the Galerkin method [2], numbers of expansion terms are set as $L=3$ and $M=10$.

Under these constraints, the relation between a_2 and a_3 is shown in Fig.3 for $\Theta_M=30^\circ, 60^\circ$, and the eigenvalues of first four modes, i.e., TE_{10} (dominant mode), TE_{20} , TE_{01} , and TE_{11} , are shown in Fig.4 for $\Theta_M=60^\circ$. In computing the active impedance of a phased array element, the total number of both TE and TM unit cell modes is chosen as 121.

Numerical Results and Discussion

The loci of active impedance of ridged waveguide phased array for $\Theta_M=60^\circ$ with parameters of $a_2/\lambda=0.25, 0.35$ are shown in Fig.5, in which scan planes are $\phi=0^\circ, 30^\circ, 60^\circ, 90^\circ$ with scan angle $0 \leq \theta \leq \Theta_M (=60^\circ)$ sampled in 20° intervals. Figure 6 shows the maximum VSWR versus a_2/λ for $\Theta_M=30^\circ, 60^\circ$. It is worth noting that those worst values occur at the edges of scan plane of $\phi=0^\circ$, i.e., H-plane. It is seen from Fig.5 that the locus of active impedance moves with increasing ϕ towards less capacitive region. The most important thing in Fig.6 is that the maximum VSWR value decreases with increasing the dimension a_2 . Increasing a_2 corresponds to increasing a_3 as in Fig.3, and then waveguide configuration becomes nearly conventional rectangular waveguide with wide "a" dimension.

On the other hand, only the dominant TE_{10} mode was employed in Figs. 5 and 6 except for the case of $a_2/\lambda=0.35$ since cutoff frequencies of higher modes decrease with increasing a_2 as in Fig.4. Comparison of active reflection coefficients between cases of different number of waveguide modes is shown in Table I. It is seen from Table I that waveguide higher modes have much influence on the aperture performance in the case of large dimension of a_2 . However, the deviation from the case of number of modes, $I=4$ is 7.4% for $a_2/\lambda=0.35$ and this is not seriously too large. Hence, employment of only the TE_{10} mode is sufficient to know the qualitative characteristics of such a phased array element in the first stage of the element design. This will also save much of the computational time.

Conclusion

From numerical results, it is concluded as follows;

- (1) Best ridged waveguide configuration for relatively narrow band use may be nearly rectangular waveguide with large "a" dimension.
- (2) The dominant mode itself will give sufficient informations on the active aperture performance of ridged waveguide phased array elements in an equilateral triangular arrangement.

References

- [1] J. P. Montgomery (IEEE Trans. AP-24, pp.46-53, Jan. 1976)
- [2] J. P. Montgomery (IEEE Trans. MTT-19, pp.547-555, June 1971)
- [3] S. S. Wang and A. Hessel (AD-A031472, chap. V, Mar. 1976)
- [4] G. N. Tsandoulas (Microwave J., pp.49-56, Sept. 1972)

Table I

Comparison of active reflection coefficients between cases of different number, I of waveguide modes ($\Theta_M=60^\circ, \phi=0^\circ$, and $\phi=60^\circ$).

a_2/λ	$I = 4$		$I=1$ (TE_{10} only)		
	$ R $	$\angle R$	$ R $	deviation	$\angle R$
0.2	0.9183	-1.06°	0.9326	1.6%	0.18°
0.35	0.7570	-56.62	0.8133	7.4	-45.08

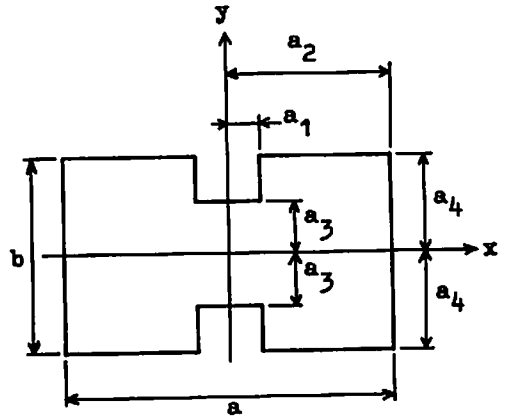
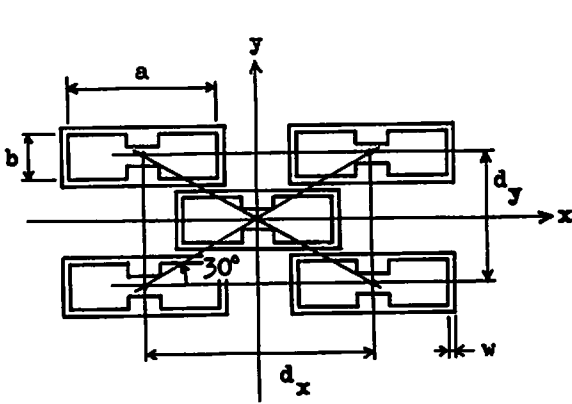


Fig. 1. Ridged waveguide elements in an equilateral triangular arrangement. Fig. 2. Geometry of ridged waveguide.

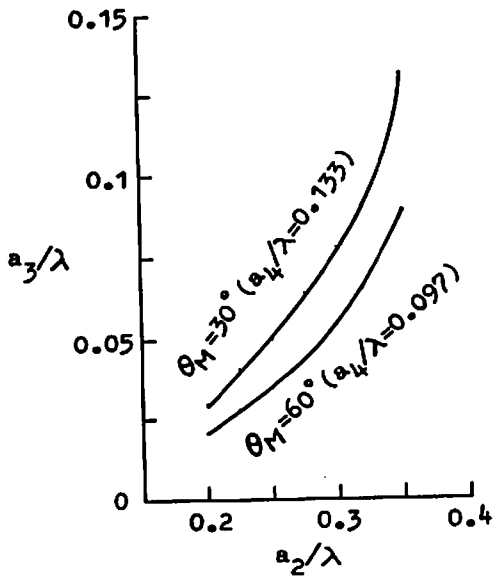


Fig. 3. Relation between dimensions, a_2 and a_3 ($f_{c1}/f=0.7$ and $a_1/a_2=0.2$).

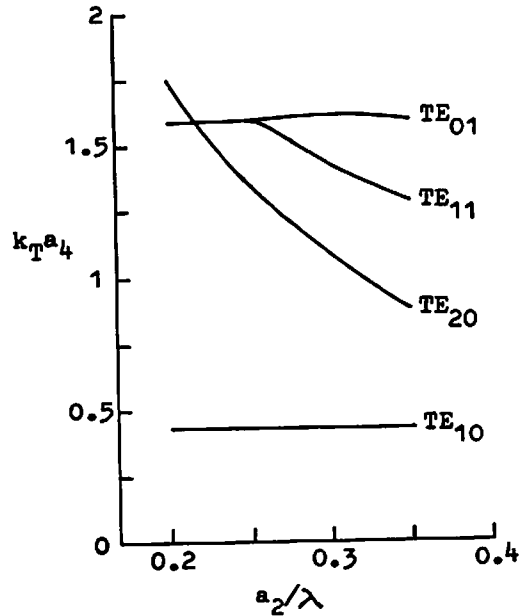


Fig. 4. Eigenvalues, k_T , of the first four modes of ridged waveguide ($\theta_M=60^\circ$, $f_{c1}/f=0.7$, and $a_1/a_2=0.2$).

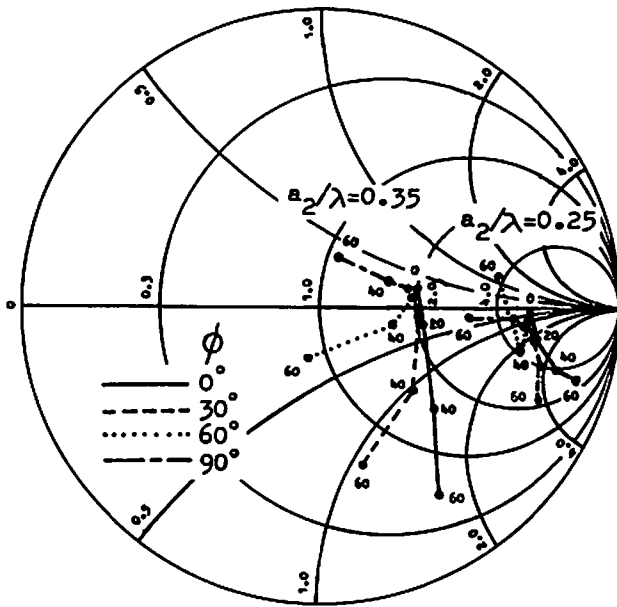


Fig.5. Active impedance of a ridged waveguide phased array ($\theta_M=60^\circ$).

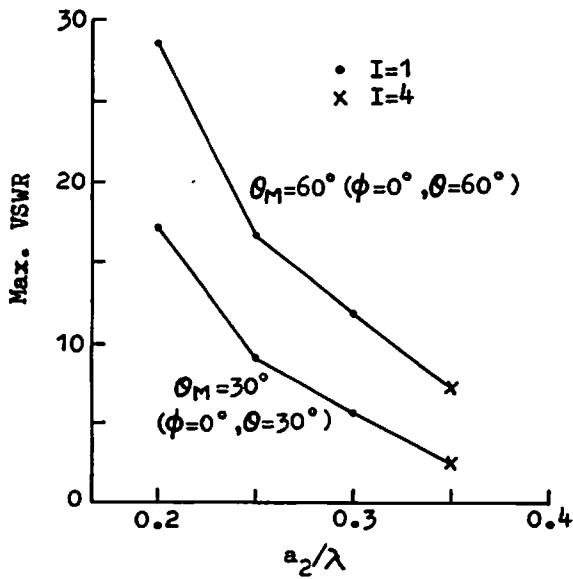


Fig.6. Maximum VSWR values of a ridged waveguide phased array.